C4R

Capacity for Rail

Towards an affordable, resilient, innovative and high-capacity European Railway System for 2030/2050

Report on demonstration of innovative monitoring concepts

Submission date: 03/10/2017

Deliverable 42.3

This project has received funding from the European Union's Seventh Framework Programme for research, technological development and demonstration under grant agreement n° 605650








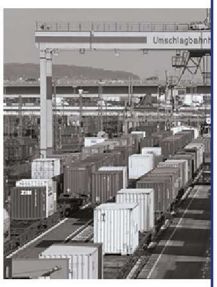

Collaborative project SCP3-GA-2013-60560
Increased Capacity 4 Rail networks through enhanced infrastructure and optimised operations
FP7-SST-2013-RTD-1

Lead contractor for this deliverable:

- UoB

Project coordinator

- International Union of Railways, UIC

1 Executive Summary

Safety on the railway is assured, or safety risks managed, by accepted inspection against standards and/or time-based maintenance methods. An asset can fail in a way that leaves the railway safe, but either operating in a degraded mode, or not operating at all. Therefore, once safety has been assured, the next concern is to improve asset performance, for example to improve capacity or punctuality, or to reduce maintenance costs by the use of timely interventions. Condition monitoring provides a means of improving the performance of an asset.

By their nature, condition monitoring systems tend to operate continually and ideally ubiquitously. Measurement systems can either be one-to-many, for example a lineside system monitoring all passing trains, or a train-borne system monitoring the track below; or condition monitoring is so low cost that it can be widely deployed: initially at the most critical places, e.g. transition zones or switches and crossings.

This deliverable focuses on a demonstration of an innovative monitoring system that is designed based on the research described in previous deliverable in work package 4.2. Key elements such as sensing, power, and communications technologies are included. It has also considered processing architectures, algorithms, and the final integration.

Technologies were first identified and screened using a technology marketplace / identification framework, developed in D4.2.1. This includes evaluation based on power consumption, sensor capabilities, scalability, environmental issues, stability, and installation and maintenance complexity. In addition to the sensing technologies, energy harvesting, energy storage, processing and communications systems are also key parts of this work. These evaluations are generally related to capacity and suitability of use within the environment. In the latter (processing and communications) cases the focus is on factors such as speed, effectiveness, bandwidth, reliability and power consumption as well as the practicalities of installation. Based on this, a range of vibration sensors and gyroscopes were assessed, and examples of laboratory and field based evaluations are provided.

Following the laboratory and preliminary field trials, a demonstrator was developed. The demonstrator consists of a lineside condition monitoring system that measures track support. The important points are: keeping the cost and power consumption to a minimum and using an energy harvesting system. The ease of installation and wireless communication are also taken into account.

Two transition zones were selected for the deployment of the demonstrator. The monitoring system consists of wireless vibration sensing nodes (locally or wirelessly powered) and a central aggregator powered by a solar energy harvester. The result was that the vertical acceleration of a sequence of concrete sleepers was recorded and uploaded to a central server. The vertical displacement was then calculated from the acceleration, showing the support provided to each sleeper. In addition, the data are passed through monitoring algorithms to identify impulses mainly introduced by defective wheels.

2 Table of contents

1 Executive Summary 3
2 Table of contents 4
3 List of Figures 6
4 List of Tables 8
5 Introduction 9
6 Objectives 10
7 Background 11
8 Technology identification 13
8.1 Track degredation 14
8.2 Sensing 16
8.2.1 Gyroscopes 17
8.2.2 Accelerometers 17
8.2.3 Sensing evaluation 18
8.3 Energy Harvesting and Storage Systems 22
8.3.1 Solar 23
8.3.2 Energy storage systems 25
8.4 Data logging and Processing 26
8.4.1 Hardware platform 27
8.4.2 Monitoring Algorithms 29
8.5 Communications 29
8.5.1 Wireless 29
8.5.2 Wired 31
9 System Integration 33
10 Field Trials 34
10.1 Transition to a tunnel – UK 34
10.2 Transition onto a bridge – Portugal 35
10.2.1 Central unit configuration 35
10.2.2 Sleeper nodes 37
10.2.3 System output 39

10.2.4 Crest factor analysis 42
10.2.5 Monitoring battery voltage 44
10.2.6 Node problems 46
11 Conclusions 48
12 References 49

3 List of Figures

Figure 1: Low power embedded processing unit including the MEMS accelerometer. 11
Figure 2: WiRailCom final demonstration. 12
Figure 3: Technology Marketplace Chart template 13
Figure 4: Technology marketplace chart for vibration sensing 14
Figure 5: System design overview. 14
Figure 6: Transition onto a bridge. 15
Figure 7: Track degradation over time 16
Figure 8: First and last recordings 16
Figure 9: Piezo vibration sensor and a potted mems accelerometer 18
Figure 10: VC20 Vibration Calibrator [7] 19
Figure 11: Vibration signals measured from Piezo and MEMS accelerometers. 20
Figure 12: Frequency analysis results from Piezo and MEMS accelerometers. 20
Figure 13: Sensors testing on a sleeper 21
Figure 14: Geophone (black) vs accelerometer IEPE (red) 22
Figure 15: Solar Power (Monthly Average) 23
Figure 16: BP Solar Panels 24
Figure 17: Steca voltage regulator for Solar Panels 25
Figure 18: Camdenboss 45Ah Gel battery. 26
Figure 19: Camdenboss 130W solar panel. 26
Figure 20: Microchip 16 bit Microcontroller. 27
Figure 21: Raspberry PI 3 28
Figure 22: Microchip ISM module 30
Figure 23: Frequency analysis for the Microchip MRF89XAM89A 30
Figure 24: TP-link MR200 4G router [17] 31
Figure 25: MR200 ethernet ports. 32
Figure 26: Overview of the system configuration 33
Figure 27: Wired accelerometer on the sleeper on HS1. 34
Figure 28: Acceleration of three sleeper on HS1 line. 34
Figure 29: Trackside system architecture 35
Figure 30: UPorto hardware configuration 36
Figure 31: UPorto hardware in wayside cabinet 37
Figure 32: UoB master receiver node 37
Figure 33: UPorto sleeper node configuration 38
Figure 34: UPorto solar harvesting sleeper node 38
Figure 35: Inside the UoB sleeper node 39
Figure 36: UoB sleeper node 39
Figure 37: Accelerations measured from UoB nodes 40
Figure 38: 2nd order Butterworth high-pass filter - Fc =5 Hz 41

Figure 39: Displacements calculated from UoB node data 41
Figure 40: Displacement caused by a high-speed Passenger train. 42
Figure 41: Displacement caused by a part of A FRIEGHT train..... 42
Figure 42: Crestogram of the vibration signal. 43
Figure 43: Vibration signal after the band-pass filter..... 44
Figure 44: Node battery voltage for each train pass for ~5 weeks 45
Figure 45: Node temperature for each train pass for ~5 weeks 45
Figure 46: Node battery voltage vs temperature..... 46
Figure 47: Node battery voltage showing sharp drop..... 46

4 List of Tables

Table 1: Piezo vs MEMS 18
Table 2: ADXL345 evaluation 21
Table 3: Geophones and vibration sensors 22
Table 4: Evaluation for solar generic panels 24

5 Introduction

In this report, the design and application of an innovative monitoring system on the railway is presented. The D4.2.1 framework and the guidance explained in the D4.2.2 report have been used in the design of the innovative monitoring system in this work.

The use of the outcomes and key points of an EC FP7 project, WiRailCom, were also considered in the design process of this project. This includes the general idea of how the system is integrated and the use of low-power and low-cost sensing technologies.

A lineside condition monitoring system that can measure track geometry is developed in this work and the following key points are included:

- Sensor and data logging system
- Low cost
- Low power
- Use of energy harvesting
- Low maintenance
- Ease of installation
- Wireless communications

The method that identifies this condition monitoring system is also explained in this report.

Appropriate sensing technologies were chosen and a number of laboratory tests have been carried out to assess the quality of different sensing technologies that can be used to monitor the track geometry.

The use of energy harvesting technologies and low power equipment are included in the design. Different communication technologies for local and remote applications are used in this work. The application of the data processing and monitoring algorithms to help identify problems are considered.

The final integration of the system and results are presented in this report. The site used to carry out the demonstration for this project is located at Alcácer do Sal, near Lisbon. The UoB has also carried out some preliminary tests on the UK high speed line (HS1) in Kent in the UK.

6 Objectives

The objective of this work is to demonstrate an innovative monitoring system identified using the D4.2.1 framework. This also uses the recommendations provided in D4.2.2 to evaluate each part of the system and finally assess the system integration.

To carry out this design the following scopes were addressed:

- Choosing the sensing technology
- Using an energy harvesting system
- Communication protocols wireless and wired
- Data recording and processing units
- Links to previous FP7 projects such as On-Time and WiRailCom

The system is also expected to be low cost, low power, robust, and intelligent.

There is a requirement for laboratory evaluation and field trial demonstration in this work, which are explained in this report.

7 Background

In D4.2.1 the use of a framework to evaluate technologies for condition monitoring system for infrastructure was designed and explained. This was followed by report D4.2.2 where the technologies were identified and evaluated. In D4.2.2, a range of sensing technologies and their applicability to the railway domain were explored, and sensor and architecture identification and evaluation techniques were demonstrated. Technologies and systems such as: signal acquisition, data processing (algorithms), power sources, energy storage solutions, communications systems and overall monitoring system architectures were described. The interactions between these system components and how they may be considered separately or in conjunction with other technologies in a design of a monitoring systems were discussed.

WiRailCom – EC FP7 Project, was to achieve a novel, self-contained, wireless and integrated condition monitoring system. The monitoring system required to contain energy harvesting, low embedded processing and wireless communications.

It was demonstrated that using bogie vibration can generate power to run a low power embedded system. A use of wireless mesh node network, using ISM 2.4 GHz band, was also a part of the demonstration. The mesh network was provided by Sencieve [1].

Low power microchip microcontroller and low power MEMS accelerometer were used in WiRailCom, shown in Figure 1.

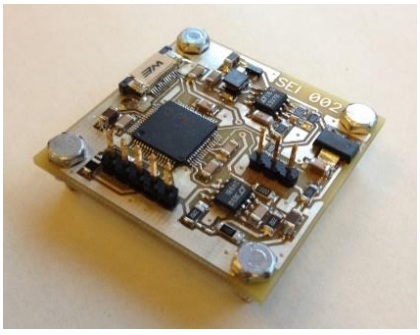

FIGURE 1: LOW POWER EMBEDDED PROCESSING UNIT INCLUDING THE MEMS ACCELEROMETER.

The embedded unit, the energy harversing system and the wireless trasmitter were installed on a test train in Long Marston, UK for final demonstration.

FIGURE 2: WIRAILCOM FINAL DEMONSTRATION.

8 Technology identification

In D4.2.2 a chart "technology marketplace", shown in Figure 3, was introduced to demonstrate technologies and their capabilities. The chart could also address the problems and motivations of each application.

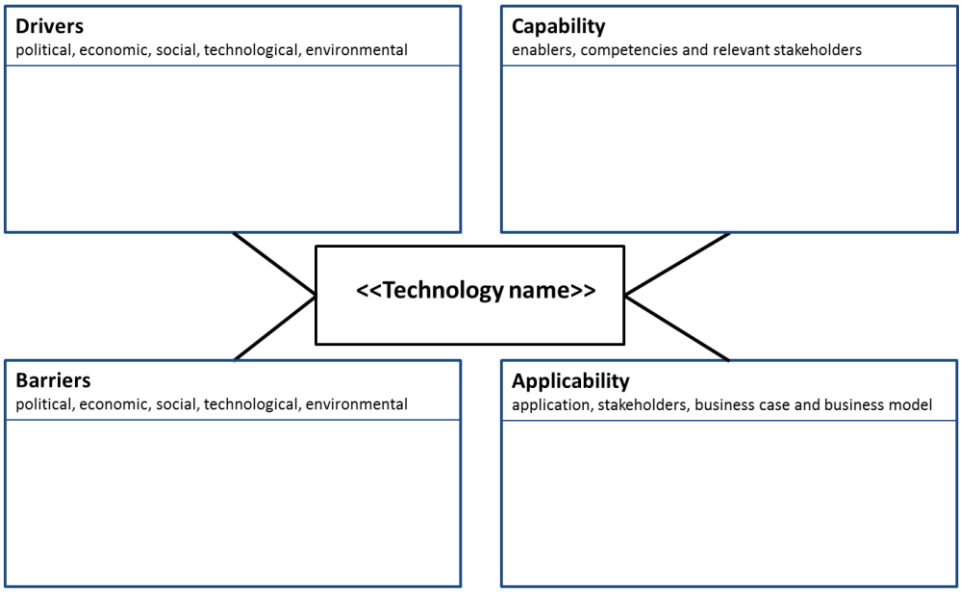

FIGURE 3: TECHNOLOGY MARKETPLACE CHART TEMPLATE

In this chart: drivers are the motivations behind each technology; capability is the requirement for the technology to be realised; barriers are the concerns that can negatively affect the technology progression and finally applicability is the application and usefulness of this technology on the railway.

Identify key requirements for inspection and monitoring systems is the first step of this work. Use of accelerometers for an application of track movement monitoring, especially the track support degradation is identified for this work. The use of technology market chart to achieve this is shown in Figure 4.

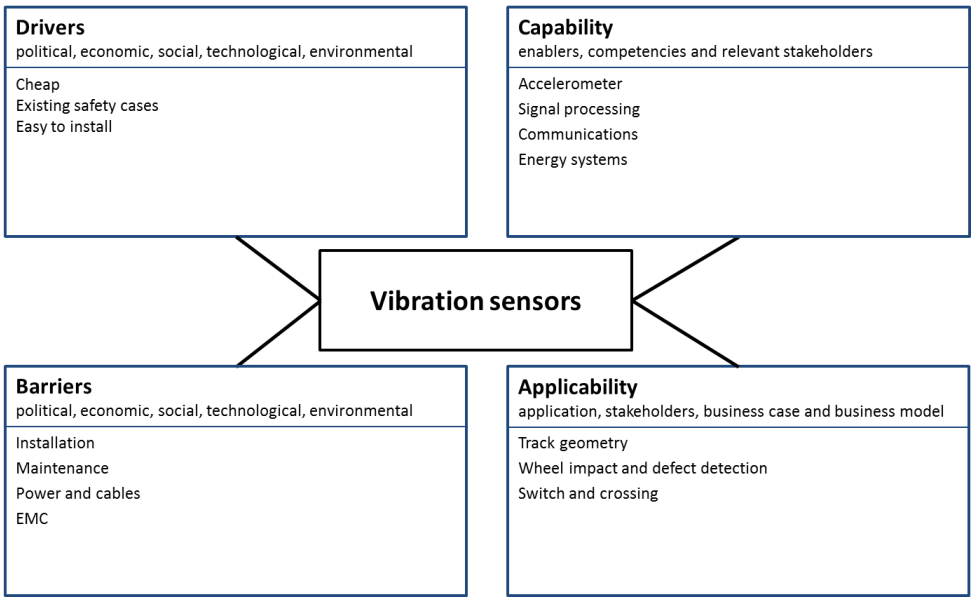

FIGURE 4: TECHNOLOGY MARKETPLACE CHART FOR VIBRATION SENSING

There are different sensing technologies to measure the movement of the track, which is investigated and assessed in this work. This work is to integrate an appropriate sensing technology, a low power processing system and a wireless communication method that are powered with an energy harvesting technology to demonstrate a lineside monitor system for track degradation, shown in Figure 5.

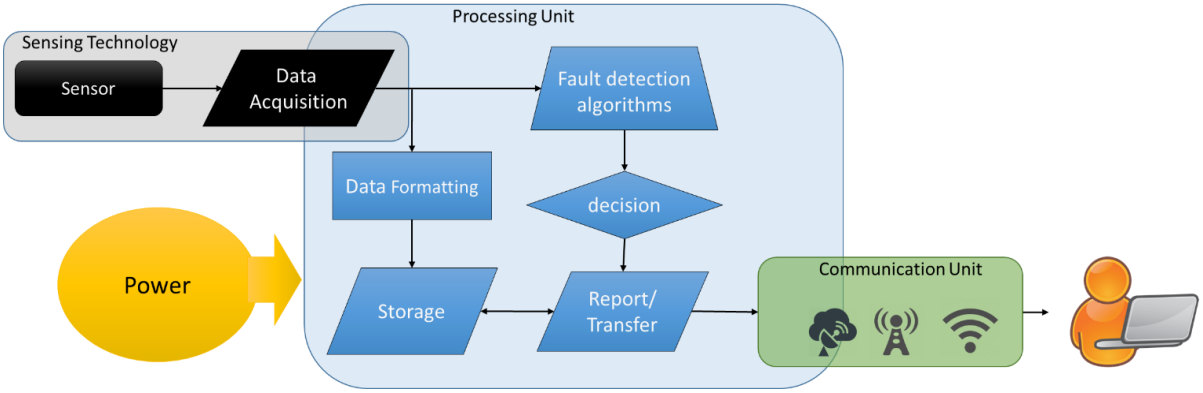

FIGURE 5: SYSTEM DESIGN OVERVIEW.

8.1 TRACK DEGREDATION

Track degradation is the process of track geometry deterioration following initial track construction or remedial work.

Railway vehicles operating on the track in various weather conditions can cause settlement and the level of support provided by ballast changes. Extremely wet or dry weather conditions, high temperatures can also cause movement of the ballast and sub-ballast. Frost heave is one example where water between the ballast particles freezes and therefore causes expansion of the support layer and resulting track movement.

One of the parameters subject to degradation is the vertical profile of the track. Degradation in the profile of track are usually caused by uneven ballast settlement which itself can be caused by a number of issues, such as wet spots in the ground and the passage of railway vehicles. This will lead to a poor passenger ride quality. Also, high levels of degradation can lead to failures such as rail cracking [2].

A use of vibration sensor to measure the track movements was previously carried out by Yeo *et al*. from the University of Birmingham [2]. Degradation of a transition zone onto a bridge located in west Sussex was examined.

FIGURE 6: TRANSITION ONTO A BRIDGE.

Data from inertial sensors mounted on the bogie of an in-service vehicle were collected. The recordings of the track geometry variations over 8 months are shown in Figure 7.

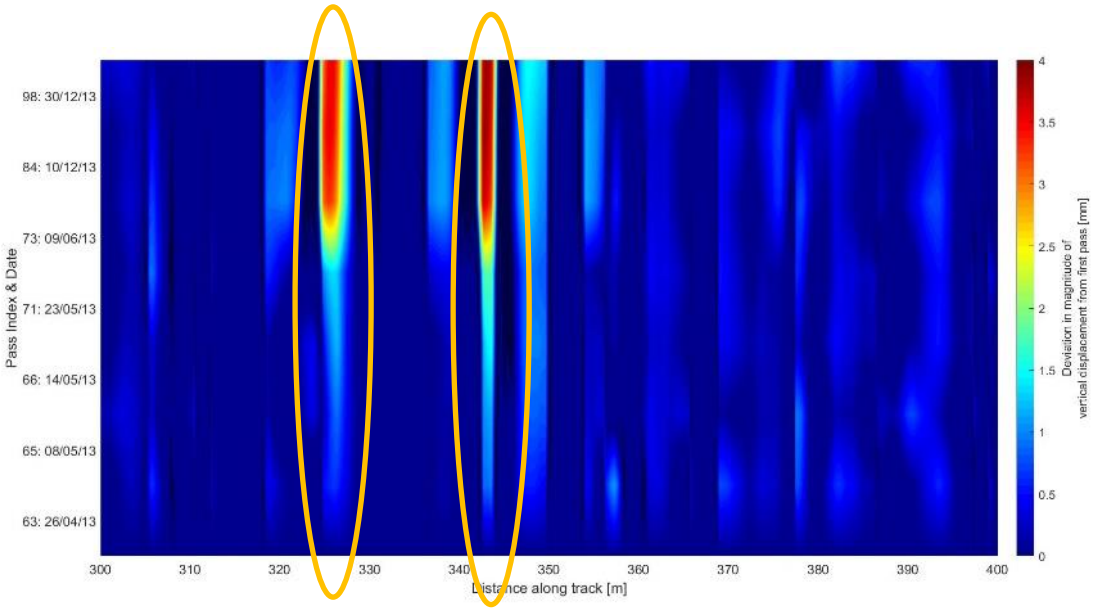

FIGURE 7: TRACK DEGRADATION OVER TIME

In the regions of Figure 7, highlighted with ellipses, the track geometry has noticeably changed over time. Figure 8 illustrates the first and the last days of the recordings from the selected areas. This shows that the track geometry is deteriorating while other geometry is technically worse, the highlighted sections are changing while the remainder is stable.

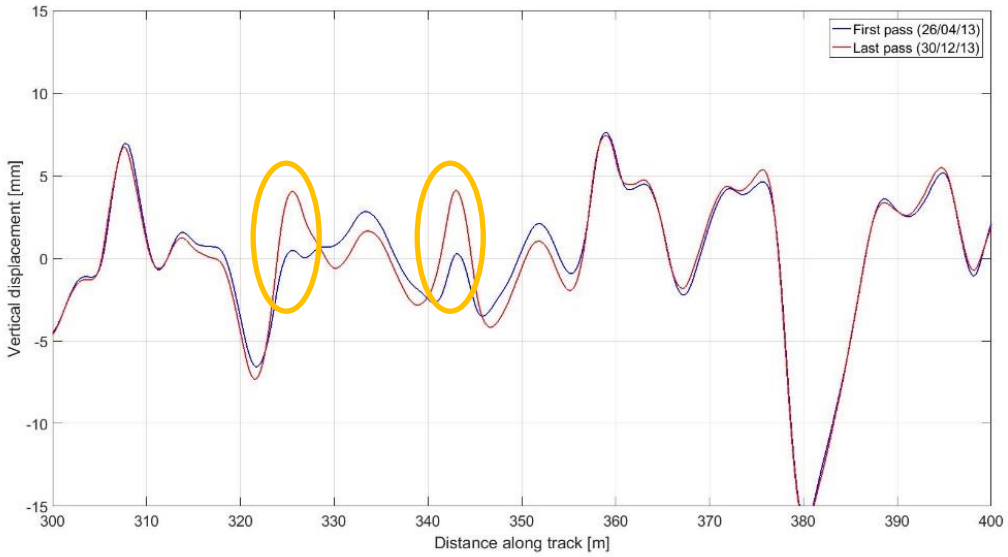

FIGURE 8: FIRST AND LAST RECORDINGS

8.2 SENSING

To monitor track geometry, sensors such as accelerometers and gyroscopes can be used. In this work, each sensor should be evaluated based on its power consumption, sensor options, scalability, environmental capabilities, stability, installation and maintenance.

8.2.1 GYROSCOPES

Gyroscopes are devices that measure rotational motion. Modern gyroscopes can be based on different technologies such as MEMS gyroscopes, ring lasers, fibre optic and quantum gyroscopes.
In terms of functionality, there are two main types of gyroscopes (or 'gyros'): angular rate gyros and angular position gyros. Angular rate gyros are able to detect rotation rate and angular position sensors can integrate the angular movement in order get the angular displacement. Until relatively recently, gyroscopes tended to be large and heavy, which limited their application. Currently, MEMS technology allowed the development of much smaller and lighter devices which are manly used in inertial measurement and navigation systems [3].

8.2.2 ACCELEROMETERS

Accelerometers are inertial sensors that sense acceleration. Using an integrated multiple-axis sensor, or a combination of three single-axis sensors, it is possible to measure in three orthogonal axes. They can be used to sense acceleration, vibration, tilt (orientation) or as an impact sensor [4].

Two main types of accelerometer are piezoelectric and MEMS (micro electromechanical systems).

The designs of the piezoelectric sensors consist of force sensitive crystal and an attached seismic mass. A preload ring applies a force to the sensing element assembly to make a rigid structure and ensure linear behaviour. Under acceleration, the seismic mass causes stress on the sensing crystal which results in a proportional electrical output. Most common piezoelectric sensors have integrated circuits that convert a high-impedance charge signal generated by a piezoelectric sensing element into a usable low-impedance voltage signal that can be easily transmitted over two wires to a data acquisition system [5].

The other type of accelerometer is the MEMS type. Microelectronic fabrication techniques are used to manufacture these sensors. The techniques create mechanical sensing structures of microscopic size, usually on silicon. MEMS sensors are used to measure acceleration when coupled with microelectronic circuits. Unlike piezoelectric sensors, MEMS sensors measure frequencies down to 0 Hz which enables gravity to be sensed. There are two types of MEMS accelerometers [6]:

- Variable capacitive (VC) MEMS accelerometers are lower range, high sensitivity devices used for structural monitoring.
- Piezoresistive (PR) MEMS accelerometers are higher range, low sensitivity devices used in shock applications.

8.2.3 Sensing evaluation

To perform the track geometry monitoring capability of some of aforementioned sensing technologies have been evaluated by the UoB.
Laboratory testing at the BCRRE and field trials at the Long Marston facility have been carried out.
A variety of different grade (cost) accelerometers have been used in this evaluation procedure.

Figure 9 demonstrates a piezoelectric and a MEMS accelerometer. The MEMS accelerometer is potted in a plastic enclosure to allow for simple mounting.

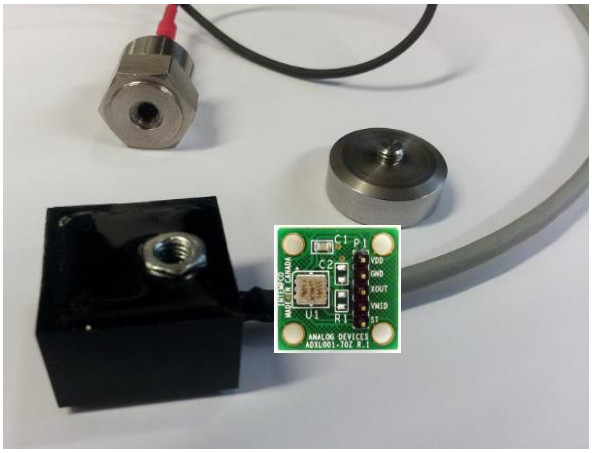

Figure 9: Piezo vibration sensor and a potted MEMS accelerometer

MEMS in average draws about 0.75 mW and the piezo current consumption is around 132 mW. Table 1 summarises the main features of these two accelerometers.

Table 1: Piezo vs MEMS

	KS76a (Piezo)	ADXL001 (MEMS)
Interface	IEPE	Voltage
Power	~ 132 mW	< 1 mW
Range	±120 g	± 250 g
Resonant frequency	> 34 kHz	22 kHz
Sensitivity	50 mV/g	4.4 mV/g
Noise	80 µg (20 – 50000 Hz)	95 mg (100 – 400 Hz)
Price	>£100	~£4
Temperature range	-20 to 120 ˚C	-40 to 85 ˚C

In order to compare the accuracy of the measurements from the sensor, a vibration calibrator was used. VC20, shown in Figure 10: VC20 Vibration Calibrator Figure 10 is a vibration calibrator and vibrates at a frequency of 159.2 Hz and RMS level of 10 m/s^{-2}.

FIGURE 10: VC20 VIBRATION CALIBRATOR [7]

Figure 11 shows the signals recorded with the both accelerometer. It is noticeable that the MEMS has a high level of noise but this is partially due to its sensitivity.

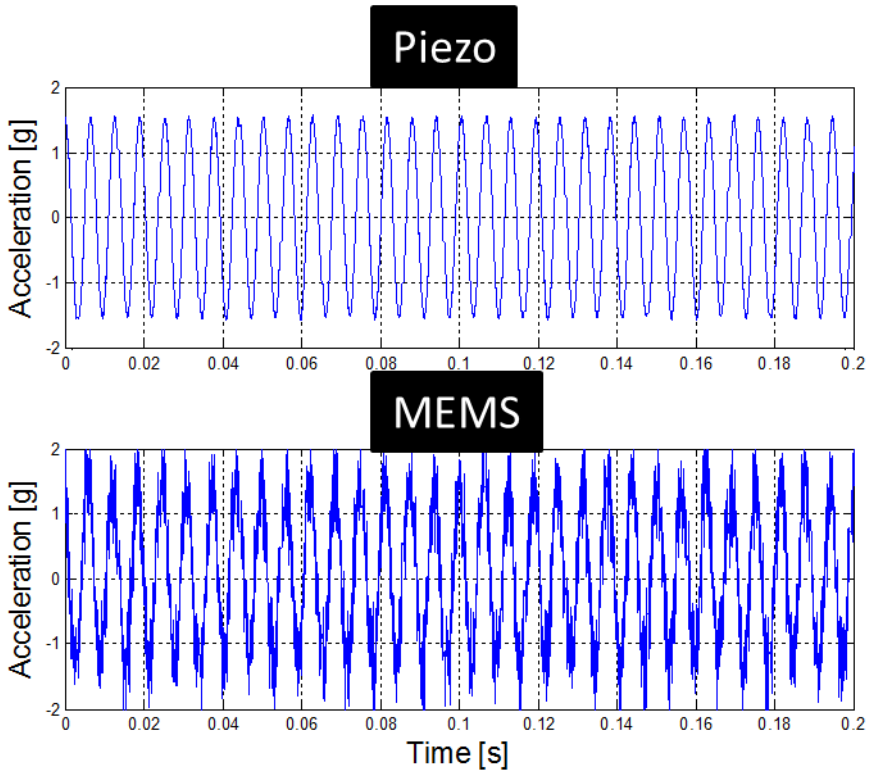

FIGURE 11: VIBRATION SIGNALS MEASURED FROM PIEZO AND MEMS ACCELEROMETERS.

To assess the quality of the data to be used in signal processing algorithms especially in frequency domain, the Fast Fourier Transform (FFT) results of the recorded signal was compared, shown in Figure 12.

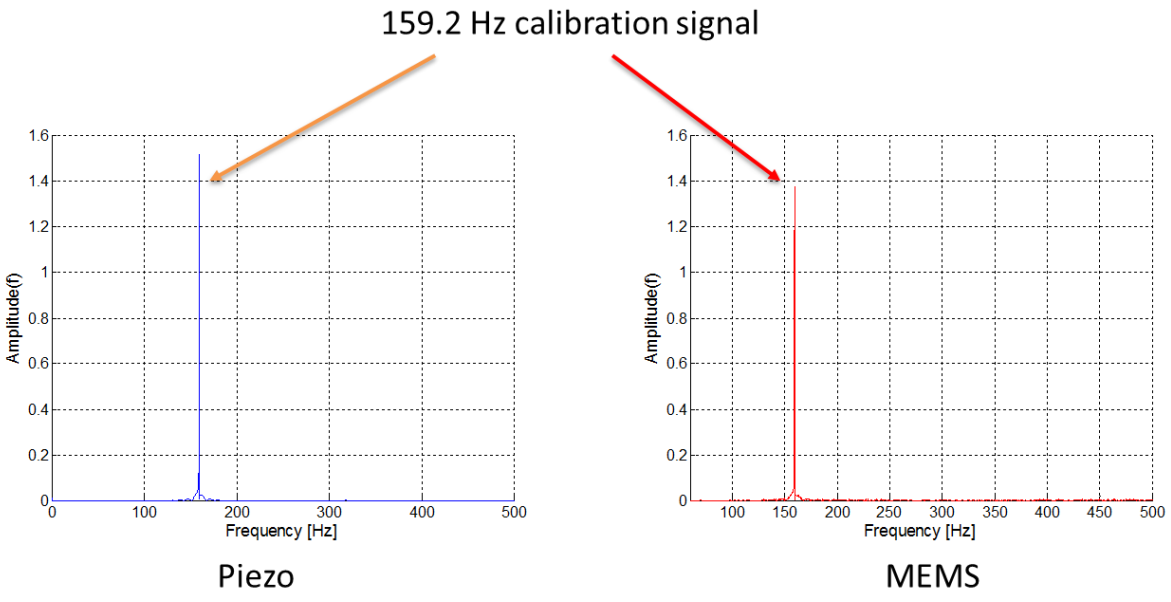

FIGURE 12: FREQUENCY ANALYSIS RESULTS FROM PIEZO AND MEMS ACCELEROMETERS.

The frequency analysis shows an acceptable match between the two sensors. An example of a more suitable and more sensitive version of the MEMS with similar cost, size and power consumption is the ADXL345. The evaluation table for this accelerometer is shown in Figure 13.

TABLE 2: ADXL345 EVALUATION

SENSORS																								
Ref Description	Automated data collection	Detection of incipient faults	Event localization	Wake up under event	Different time for sensing/sending	Scalability	Environmental compatiblity	Data collection at line speed	Different measurement modes	Custom reporting of parameters	Custom fault detection rules	Custom submision rate of measurements	Self-diagnostic	Long term stability	Long term robustness and reliability	Calibration	Geometrical compatibility	Compatibility with track maintenance	High availability on component level	High availability on sensor node	Resistance to electromagnetic fields	Mounting simplicity	**SENSOR SCORE**
WEIGHT	5%	5%	5%	5%	5%	5%	5%	5%	5%	5%	5%	5%	5%	5%	5%	5%	5%	5%	5%	5%	5%	5%	
S1 MEMS Accelerometer ADXL345	10	10	10	10	10	5	10	10	0	0	10	10	0	10	10	5	10	10	10	10	10	5	**8.0**

This accelerometer communicates using a serial protocol, SPI, to transmit data. This protocol can be easily handled by microcontroller and microprocessors.

A set of tests was carried out, by the UoB, to evaluate the quality of the measurements to assess these sensors. Figure 13 shows the test set-up configuration.

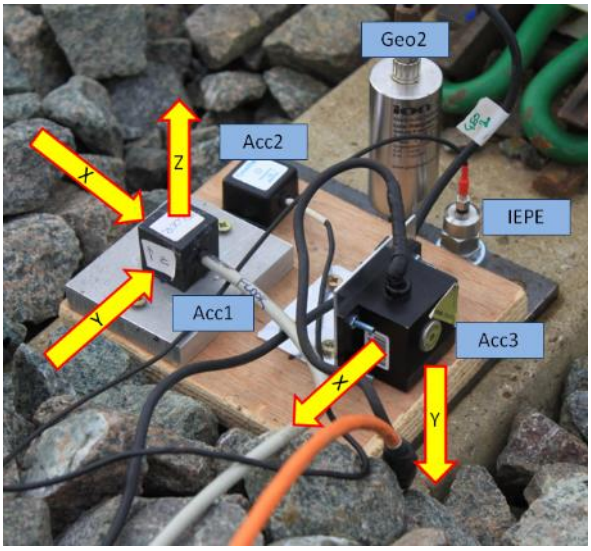

FIGURE 13: SENSORS TESTING ON A SLEEPER

Table 3 is a list of the geophone and vibration sensors use in the tests.

TABLE 3: GEOPHONES AND VIBRATION SENSORS

Channel	Technology	Model	Description	Range	Sensitivity	
2	Geophone	LF-24	Geo 2	NA	15	V/(ms^{-1})
5	Accelerometer	ADXL 103	Acc1 - X,Y,Z	1.7 g	1000	mV/g
8	Accelerometer	CXL04	Acc2 - Z	4 g	500	mV/g
9	Accelerometer	CXL10TG3	Acc3 - X,Y	10 g	166.66	mV/g
11	Accelerometer	KS76(a)	IEPE	120 g	50	mV/g

Figure 14 illustrates the results of the vertical speed. It shows that the accelerometer has a minor drift over time (this can be compensated using post-processing algorithms). Apart from the drift demonstrates a good similarity between the two sensors. The accelerometer, CXL04LP1Z, is about ten times cheaper than the geophone. This shows that a cheap vibration sensor with some pros-processing algorithms can achieve the same results instead of an expensive geophone.

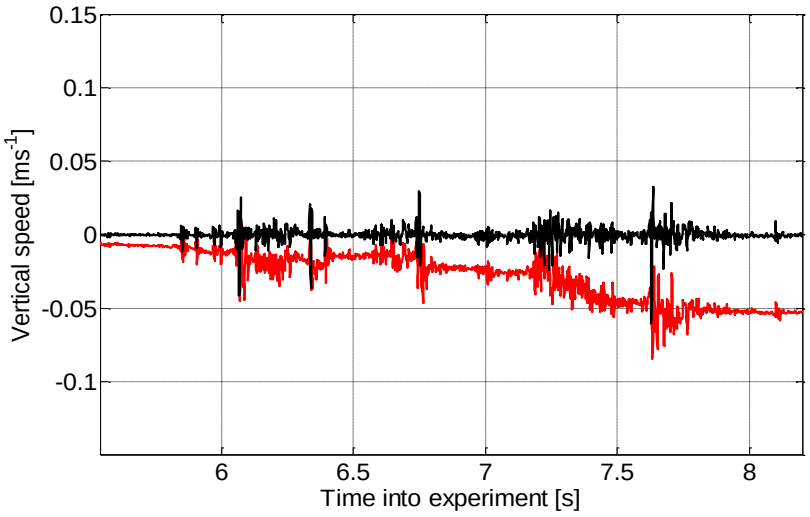

FIGURE 14: GEOPHONE (BLACK) VS ACCELEROMETER IEPE (RED)

8.3 ENERGY HARVESTING AND STORAGE SYSTEMS

Energy harvesting is a smart technique for a wide variety of self-powered micro-systems. Wireless sensor networks are a good example of such systems which require little or no maintenance.

The use of energy harvesting in railways will reduce the need for running cable around the infrastructure. Thus, reducing some of the cable related maintenance problems. This will also ease the installation of new monitoring systems, especially at the locations where there is no access to the grid

such as railway bridges. Therefore, a key challenge for the successful deployment of energy harvesting technology remains, in many cases, the minimisation and management of the energy used [8].

8.3.1 Solar

Modern solar power systems have a variety of uses in off-grid applications to provide electrical power at sites where the grid is inaccessible or too costly.

Photovoltaic (PV) cells are one of the most mature energy harvesting technologies. They are widely used to provide power to homes and businesses, as well as electronic devices, including sensors. PV cells are made from different semiconducting materials, including various forms of silicon such as monocrystalline, polycrystalline and amorphous, as well as other different compounds. Each of these have different kinds of energy conversion efficiency, defined as the ratio of the incident solar power to the electrical power generated. Cell efficiencies can vary from 6% for amorphous silicon to a little over 40% for multiple-junction research cells [9] [10]. Typical single-junction silicon cells produce approximately 0.5-0.6V and they are usually connected in series to provide voltages usable with electronic circuitry.

Where sensors will be placed at outdoor locations, a small solar panel can be a good way to provide power. The voltage and current levels can easily be matched with microelectronics and they have a relatively consistent efficiency over a broad range of wavelengths.

Using solar panels, the energy is delivered for only part of the day and it also depends on latitude and atmospheric conditions. Power outputs for different conditions are shown in Figure 15, where the power output from a 10 x 5 cm solar panel with 13% efficiency is represented as a monthly average.

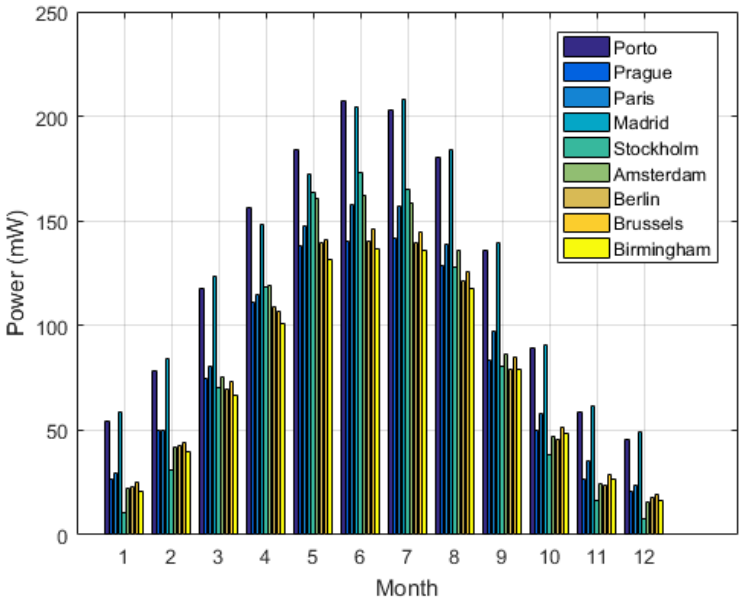

Figure 15: Solar Power (Monthly Average)

For places such as Stockholm or Birmingham with less favourable latitudes and prevailing weather conditions, the generated power can still be enough for a low power trackside monitoring system. Sufficient power can be provided by choosing the correct size solar panels together with an appropriate energy storage system. The energy storage saves excess energy when solar power is abundant and releases it when solar power is not available.

The location used for the field trial in this report, Alcacer de Sal in Portugal has an excellent solar power potential similar to that in Porto.

BP Solar panels, shown in Figure 16, are photovoltaic modules that can be used in conjunction with batteries and wind turbines. These can produce up to 20W and the maximum size is about 500x600x50 mm [11].

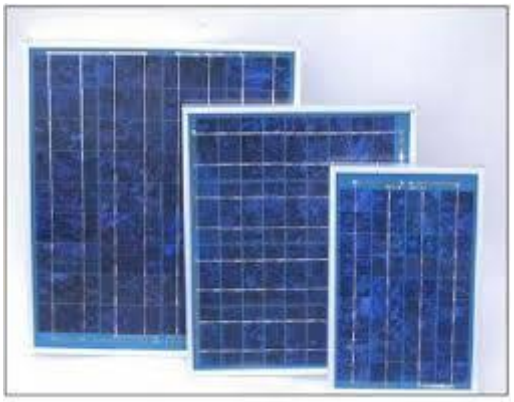

FIGURE 16: BP SOLAR PANELS

TABLE 4: EVALUATION FOR SOLAR GENERIC PANELS

ENERGY HARVESTING								
Ref	Description	Suitability for installation at different sites	Monitoring and reporting of battery status	Self-diagnostic	Environmental compatiblity	Resistance to electromagnetic fields	Mounting simplicity	ENERGY HARVESTING SCORE
	Weight	17%	17%	17%	17%	17%	17%	
E1	Solare panel BP SX20U	5	5	0	5	10	10	**5.8**

Solar and similar energy harvesting technologies usually are used in combine with battery systems. However, the outputs of these technologies need specific power electronic circuits to make the

outputs suitable for charging batteries. Figure 17 is the power electronics that regulates the voltage outputs for appropriate battery charging in this demonstration [12].

FIGURE 17: STECA VOLTAGE REGULATOR FOR SOLAR PANELS

8.3.2 ENERGY STORAGE SYSTEMS

To obtain standalone systems, energy storage is the key component for creating sustainable energy systems. Solar photovoltaic can generate energy in a sustainable and environmentally friendly manner; yet their intermittent nature still prevents them from becoming a primary energy source. However, the use of this technology required suitable geographical locations which needs to be considered. Energy storage technologies have the potential to offset the intermittency problem of renewable energy sources by storing the generated intermittent energy and then making it accessible upon demand.

8.3.2.1 LEAD-ACID

This is a mature technology, especially with the experience gathered from decades of use in the automotive and rail industries.

One of the more modern types of lead-acid batteries is AGM (absorbed glass mat). AGM is a special glass mat design that aims to wick the battery electrolyte between the battery plates. AGM batteries contain enough liquid to keep the mat moist with the electrolyte and if the battery is broken no free liquid is available to leak out.

Another type is the Gel Cell which contains a silica gel that the battery electrolyte is held in; this thick paste shape material allows electrons to flow between plates and will not leak from the battery if the case is broken.

Both batteries have similar characteristics; such as deep cycle, low self-discharge, safe for use in areas with limited ventilation systems, and they can be transported safely without requiring any special handling or being spilled. These batteries are maintenance free.

AGM is preferred when a high burst of current are required. Gel Cell batteries are usually more expensive and do not offer the same power capacity as the same physical size AGM batteries. The Gel

Cell batteries have slow discharge rates and slightly higher ambient operating temperatures. One of the drawbacks of the Gel Cell is that they must be recharged correctly or the battery will fail. The battery charger being used to recharge the battery(s) must be designed or adjustable for Gel Cell Batteries with special regulators. Gel cell batteries also have a greater life expectancy [13].

Gel batteries are suitable for repeated cycling and heavy discharge circumstances. They are also resistant to freezing. These types of batteries are currently used in conjunction with wind, solar and other energy harvesting systems [14].

Figure 18 is an example of a gel battery that is also used in this work. If the system that is powered by this battery is about 12W then it can be run for nearly 2 days without any solar power.

FIGURE 18: CAMDENBOSS 45AH GEL BATTERY.

A 130W, shown in Figure 19, solar panel has been selected to provide power at the demonstration site. This can provide enough power, during the day, to run the system and keep the batteries fully charged at the same time.

FIGURE 19: CAMDENBOSS 130W SOLAR PANEL.

8.4 DATA LOGGING AND PROCESSING

Data storage is a vital and simple requirement of the condition monitoring systems. Every monitoring system requires the storage of data. Data storage and retrieval methods are an important aspect of monitoring systems. Current approaches are either a local storage system, where sensor data is stored

locally on each sensor node, or remote storage on base stations. Since sensor nodes have small storage capacity, low computing power and limited energy, the traditional network and data storage and retrieval solutions cannot be used. In fact, in a typical wireless sensor application, the radio transmission consumption of sensors dominates the total energy consumption. So, raw data can be processed or compressed locally to the sensor to reduce the amount of data to be transmitted.

Advances in embedded microprocessor designs have enabled the creation of low-power sensing nodes. These sensing nodes usually consist of sensing modalities such as temperature or vibration. The nodes are typically of small physical dimensions and operated by battery power and/or some energy harvesting. These nodes can become of part of a bigger network system, a sensor network, and transmit data through other nodes or share the data processing to save power and time. This means that the energy consumption is an important issue. For example, failure of a node in a sensor network due to energy consumption can lead to a loss of some information. There are methods to save energy such as conserving energy in a sensor node is to aggregate packets along the sensor paths to reduce overhead in data transmission [15].

8.4.1 HARDWARE PLATFORM

A wireless sensor network includes sensor nodes and at least one base station. Both, sensor nodes and base station include a processing unit with different processing power and computational requirements.

In this work, to acquire data from the vibration sensor, a 16-bit low power and low cost processor was chosen, shown in Figure 20.

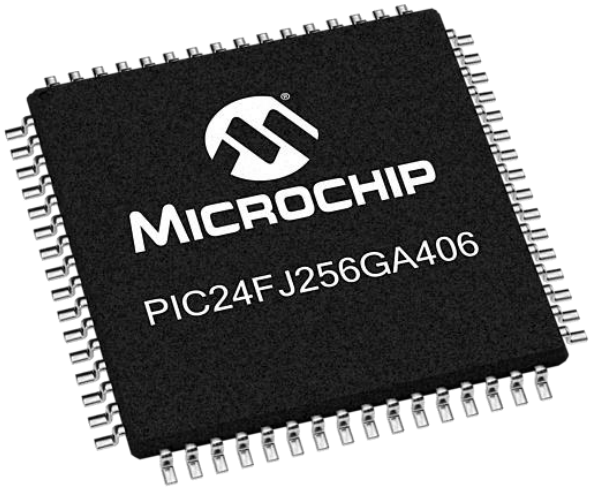

FIGURE 20: MICROCHIP 16 BIT MICROCONTROLLER.

The Microchip PIC24 is 16 Bit processing unit that is extremely low power, provides a range of digital input and output and communication buses such as SPI that can be used to communicate with a MEMS accelerometer. The main features of this processing units are:

- Low cost
- Easy to integrate with the sensor
- Can score enough using the framework
- Low power
- Capability for communication modules
- Suitable processing power and data storage
- Wide temperature range
- Easy to program using C language

Usually, sensor nodes have limited processing speeds and storage capacity with low power requirements. On a high-speed rail, where the train speed is around 200 kph or above a 6 car passenger train passes a point on the track in around 3 to 4 seconds. The chosen microprocessor can record up to 12 seconds at 1600 Hz sampling rate.

The data is recorded locally and when the train has passed, the nodes can transmit their collected data in turn. This is a time-division multiplexing method.

In this work, a trackside master node is designed to receive the locally recorded data from each node and to store them on an SD card. It also uploads the data to a remote server via a mobile phone link.

Currently commercialised low cost embedded systems such as the Raspberry PI, Arduino and development tools provided by electronic manufactures can be used for small scale monitoring and processing systems.

The Raspberry PI model 3 has been used in the design of the master node for this work, shown in Figure 21.

FIGURE 21: RASPBERRY PI 3

The system is cheap, low power, and can operate in a wide temperature range. It also has enough processing power to run algorithms for the monitoring purposes.

8.4.2 Monitoring Algorithms

The aims of the monitoring algorithms are to:

- reduce the cost of maintenance
- achieve early fault detection and prediction applications
- provide performance optimisation and improvements in reliability

A simple method to estimate the vertical displacement of the sleepers using acceleration is to double integrate with respect to time, shown in the equation below.

$$\iint a(t)dtdt = x(t) + c$$

where a is the vertical acceleration, t is time, and x is the vertical displacement. This method also generate an error, c, known as a drift. This drift is usually large due to double integration that has infinite DC gain, which acts as second order low-pass filter. Small measurement errors or offset from zero acceleration conditions accumulates after integration process. To reduce this error, a high-pass filter can be applied [2].

8.5 Communications

A range of technologies were presented in D4.2.2, which allows one to choose the appropriate wireless and wired communication technologies that could fit with the requirements for this work. The wireless communications are to be used for external access where the embedded system or the sensing node is required to transfer information to the central system or other wireless systems. The wired communication technologies are used for internal electronic systems, such as processors to wireless the module and to the sensors.

8.5.1 Wireless

Low power wireless technologies are used in this work. In this section, their related standards and the use of frequency channels and performance are explained.

8.5.1.1 Short Range - ISM band – 868/915 MHz

The industrial, scientific and medical (ISM) radio bands are radio reserved internationally for the use of radio frequency (RF) communication for industrial, scientific and medical applications. This band is also used for heating RF energy, such as found in microwave ovens.

ISM bands have also been shared with (non-ISM) license-free error-tolerant communications applications such as wireless sensor networks in the 868/915 MHz i.e. short range devices) and 2.450 GHz bands, as well as wireless LANs and cordless phones in the 915 MHz, 2.450 GHz, and 5.800 GHz bands.

The short range ISM band (~900 MHz) are usually designed for low power low baud-rate system to cover a short distance. The range can be vary from a few metres to a couple of hundred metres and the power consumption is directly related to the usable communication distance.

For low power, stand-alone trackside monitoring systems this technology is useful as it is low power and can easily be driven by energy harvesting systems or normal AA size batteries and cost efficient compared to other wireless technologies.

MRF89XAM8A, made by Microchip, is a radio transceiver module that is used for local data transmission, shown in Figure 22. Each node is equipped with this module. The data will be transferred after every measurement of a passing a train. For a passenger train with 6 cars, it takes 4 seconds to transmit the data. The system power consumption is less than 100 mW [16].

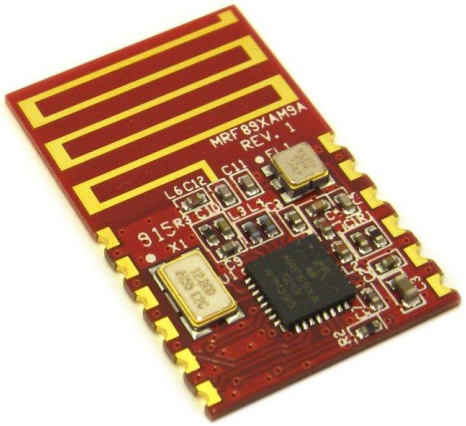

FIGURE 22: MICROCHIP ISM MODULE

Figure 23 demonstrates the fundamental frequency at which the module operates.

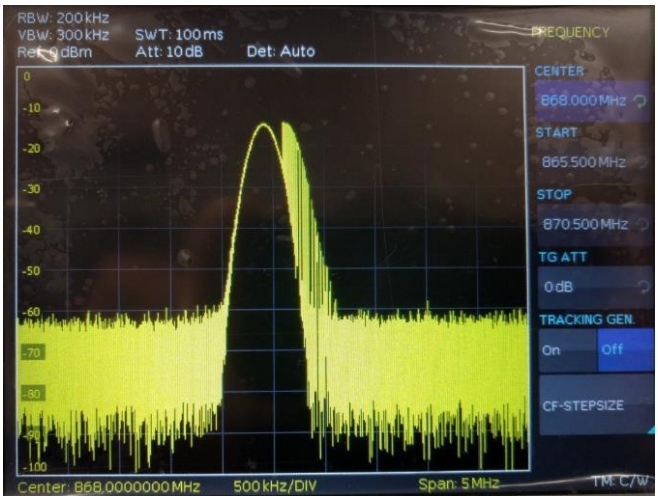

FIGURE 23: FREQUENCY ANALYSIS FOR THE MICROCHIP MRF89XAM89A

8.5.1.2 CELLULAR

To transmit the data and remote monitoring the equipment, a cellular system is used. In D4.2.2 3G and 4G technologies were introduced. Currently these systems are reliable and cost-effective. The maximum data rate be as high as 100 Mbps in 4G networks or about10 Mbps in 3G networks. In Europe, the 1900 MHz frequency band is used, which does not interfere with the short range ISM at 900 MHz.

To connect the trackside monitoring system to the internet, a 4G router (TP-Link MR200) shown in Figure 24, is used. This router has wired and wireless communication for local networks.

FIGURE 24: TP-LINK MR200 4G ROUTER [17]

8.5.2 WIRED

This part, explores the communication methods that are used in sensing and digital communication for transferring data using physical connections.

8.5.2.1 SPI

Serial Peripheral Interface is a license-free synchronous communication technique that carries a clock signal and two data lines. This method is usually used for microcontroller/microprocessors to communicate with their peripherals. SD-cards, analogue to digital convertors and serial RAMs are the common devices that use SPI.

This interface is highly sensitive to noise and requires consideration during system design for optimal performance. Over long distances, the cable introduces propagation delay, therefore without extra line drivers it is not recommend to use this method outside of printed circuit boards.

In this work, the microcontroller communicates with the accelerometer and the ISM wireless module using SPI.

8.5.2.2 UART

Universal asynchronous receiver/ transmitter (UART) is an asynchronous serial standard that originally used for telecommunication systems such as modems with specific voltage levels known as RS232. RS232 is also commonly used for low-speed industrial serial link application. The recommended maximum length is about 15 meters and maximum speed is about 2 Mbps, this can be extended using signal repeaters.

The GPS module that it is used for time synchronisation uses 5V UART method to transmit the GPS data to the Raspberry PI.

8.5.2.3 ETHERNET

Ethernet is a computer based network. TCP/IP is one of the common techniques that used for communication in this system. The network require a unique identification number for each device. The speed on this network varies from 10 Mbps to 1 Gbps. About 100 m would be the maximum length from one node to another using CAT5/CAT6 cables in this protocol [18].

In this work, the LTE router provides Ethernet ports, shown in Figure 25. This is used for local communication between the Raspberry PI and the internet. Using Ethernet instead of WiFi saves power and avoids any potential interference.

FIGURE 25: MR200 ETHERNET PORTS.

9 System Integration

In this section, the final system arrangement for the selected technologies are presented. The system is divided in two parts: central unit and sensing nodes.

The sensing nodes include the accelerometer, the PIC microcontroller and the short range ISM wireless module. These nodes are powered by a set of alkaline batteries that have low rate self-discharge. This unit has also been equipped with a temperature sensor that can to explore the effect of the ambient temperature on the battery life. The system is configured to wake up every 200 ms. If the vibration level exceeds the threshold (which is selectable remotely) the node will start sampling the acceleration signals at 1600 Hz for a maximum of 11 s. Each node will then be assigned a specific timestamp to transmit the recorded data to the central unit.

The accelerometer is wired to the microcontroller unit (MCU) using a serial protocol, SPI. The MCU also communication to the wireless module using the same serial protocol. The battery voltage and temperature will also be reported after each recording.

The central unit includes the embedded processing system, Raspberry PI, a short range ISM module, a GPS module and a 3G/4G router. The short range ISM module is to communicate with the sensing nodes and the GPS module is to assure that the time is always updated. The 3G/4G router provides internet/remote access to the embedded system and also allows the system to upload the recorded experiments and the results to the cloud.

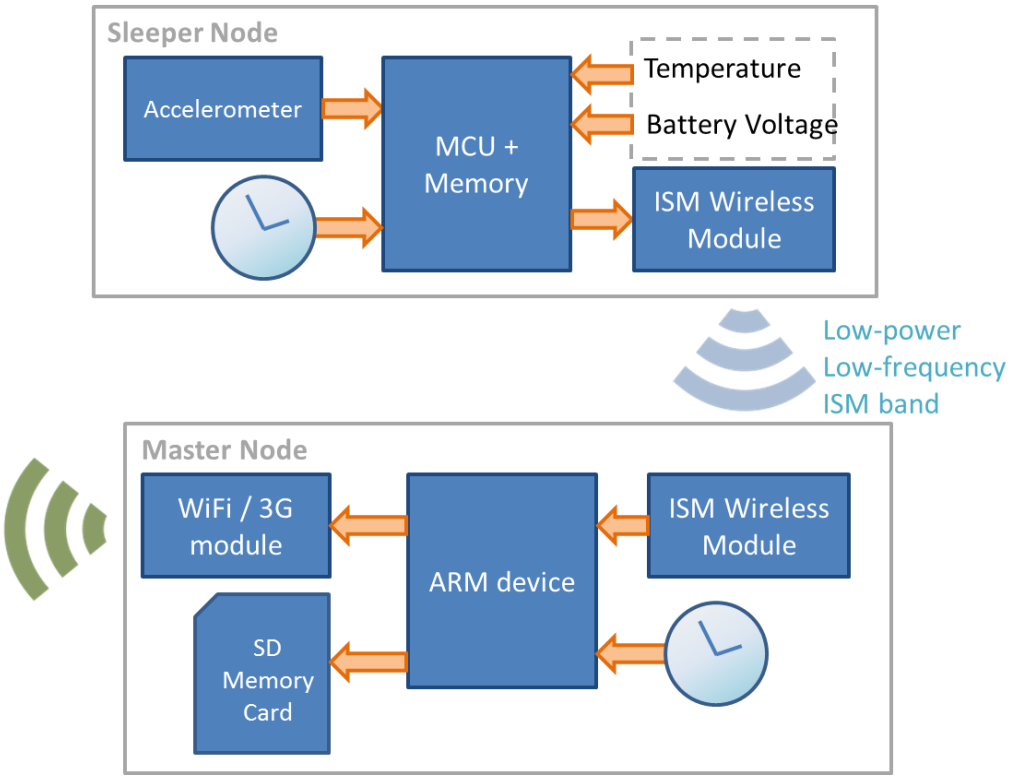

FIGURE 26: OVERVIEW OF THE SYSTEM CONFIGURATION

10 Field Trials

10.1 Transition to a tunnel – UK

The UoB has carried out a set of preliminary tests in the UK to monitor the vertical vibration of a number of sleepers of the UK high-speed one (HS1) line, shown in Figure 27. Three wired accelerometers were used to determine the minimum requirement of a low power acceleration monitoring system.

Figure 27: Wired accelerometer on the sleeper on HS1.

Displacement curves for the three accelerometers are shown in Figure 28. One of the signals is larger than the other two, which indicates that the sleeper is not supported as well as the other two.

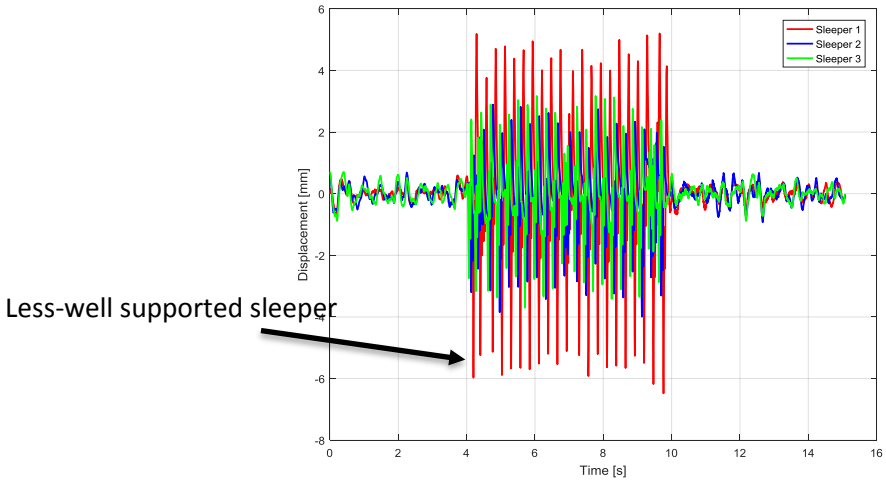

Figure 28: Acceleration of three sleeper on HS1 line.

10.2 TRANSITION ONTO A BRIDGE – PORTUGAL

Two systems were developed to measure sleeper deflection on a high-speed railway line in the Alcácer do Sal region in Portugal. The site chosen was at the transition onto a railway bridge which crosses the River Sado. The two systems both demonstrate different methods of providing wireless measurement nodes fixed to the track.

The system architecture is shown in Figure 29.

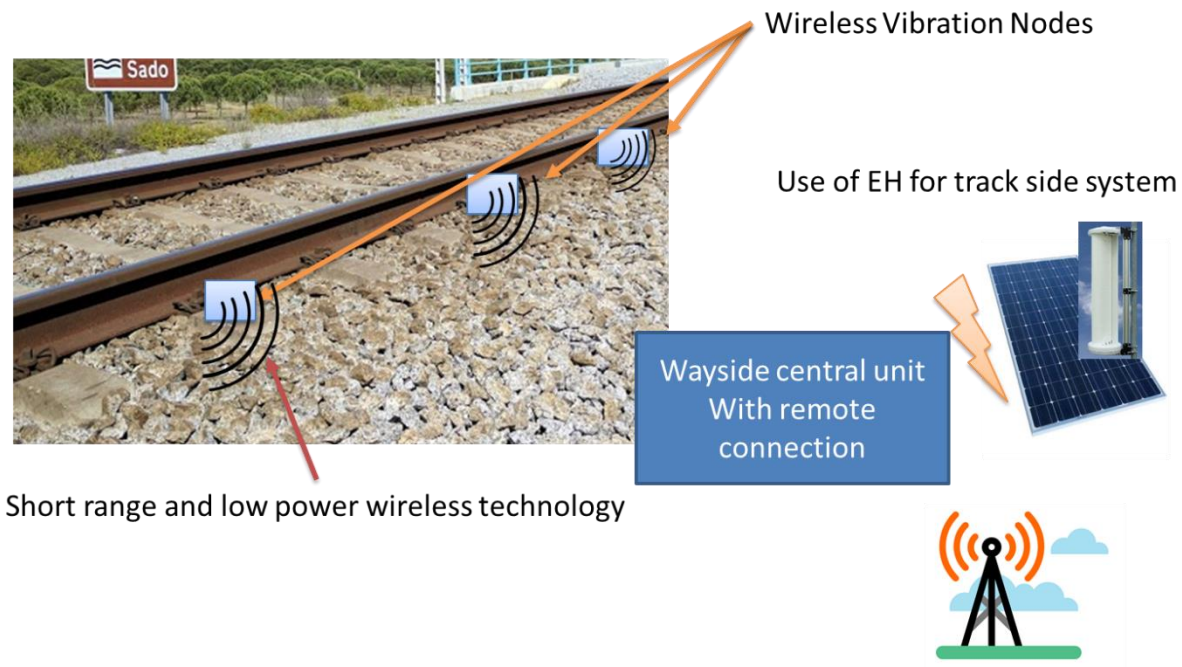

FIGURE 29: TRACKSIDE SYSTEM ARCHITECTURE

To operate without a wired power connection, the sleeper-mounted nodes must nominally operate with extremely low power consumption. Powering methods explored included batteries, energy harvesting (such as solar power), and wireless power. To keep power consumption to a minimum, both systems use short-range wireless communications to relay data to a central base station situated a few metres away from the track. The central unit collects data from the sleeper nodes, and relays it via a longer range communications method, in this case 4G. The central unit is able to do this, as it is powered by a much larger solar energy harvesting (EH) system which maintains charge in two high-capacity batteries.

10.2.1 CENTRAL UNIT CONFIGURATION

Figure 30 shows the configuration of parts within the UPorto central unit. The solar panel, mounted on a post outside the main cabinet, is connected to a solar charge controller, which maintains charge within the batteries, and provides a constant 12 V supply to the equipment within the cabinet. The

UPorto system comprises of a data receiver for collection of data from the sleeper nodes, and a small-format PC which stores the received data and makes it available via a 4G router with an internet connection.

The UoB system operates from the same power supply, and uses the same internet connectivity. The UoB master node itself contains a receiver for short-range communications from the trackside nodes, as well as an ARM computer, which stores the received data locally onto an SD card, applies simple processing algorithms and uploads received data to a remote web server.

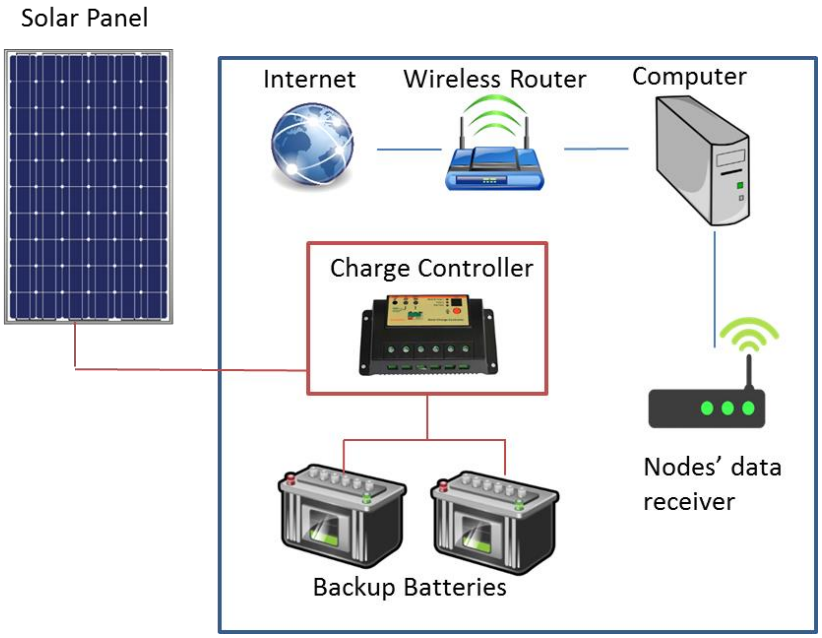

FIGURE 30: UPORTO HARDWARE CONFIGURATION

Figure 31 shows the inside of the central unit cabinet, detailing the individual components of the UPorto system. Figure 32 shows the UoB master node which is mounted externally on top of the main cabinet.

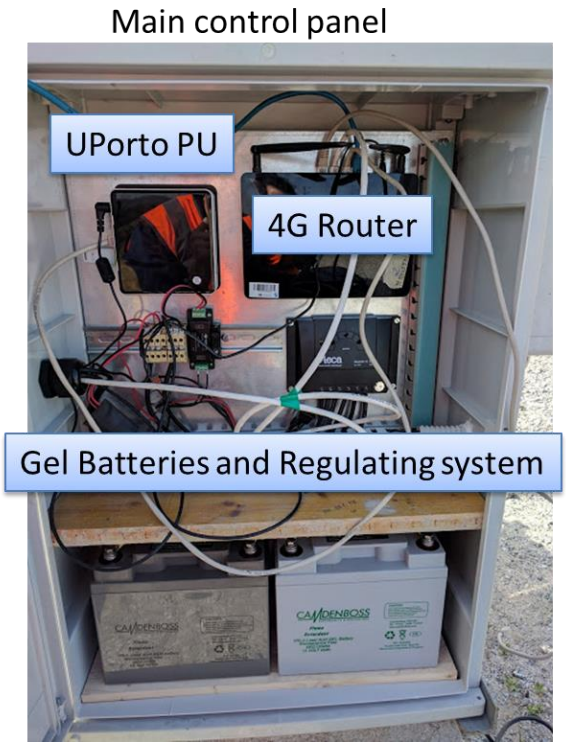

FIGURE 31: UPORTO HARDWARE IN WAYSIDE CABINET

FIGURE 32: UOB MASTER RECEIVER NODE

10.2.2 SLEEPER NODES

10.2.2.1 UPORTO NODES

The UPorto sleeper nodes, comprise internally of several modules, shown in Figure 33. The energy harvesting (EH) module, takes power generated from the wireless power receiver module. It also has integrated solar panel. Moreover, it is equipped with a lithium Ion battery, which is charged when

excess power is available from the energy harvesting sources. The EH modules supply 5 V and 3.3 V to the main board, which includes the accelerometer, short-range wireless transceiver, and the main microcontroller.

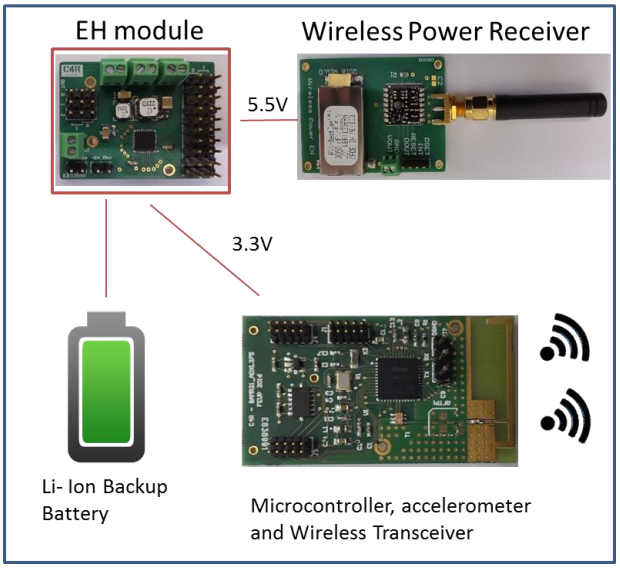

FIGURE 33: UPORTO SLEEPER NODE CONFIGURATION

The modules are contained within enclosures small enough to fit on the end of a railway sleeper. Each node is fixed to the sleeper using a waterproof adhesive. Figure 34 shows a solar energy harvesting node attached to the end of a sleeper.

FIGURE 34: UPORTO SOLAR HARVESTING SLEEPER NODE

10.2.2.2 UOB NODES

The UoB nodes operate entirely from a pair of low-cost AA batteries, and are designed to operate with extremely low power to allow the batteries to last for several years without replacement. Figure 35 shows the inside of the UoB node, showing the batteries on top of the circuit board, and the accelerometer, transceiver, and accelerometer on the underside.

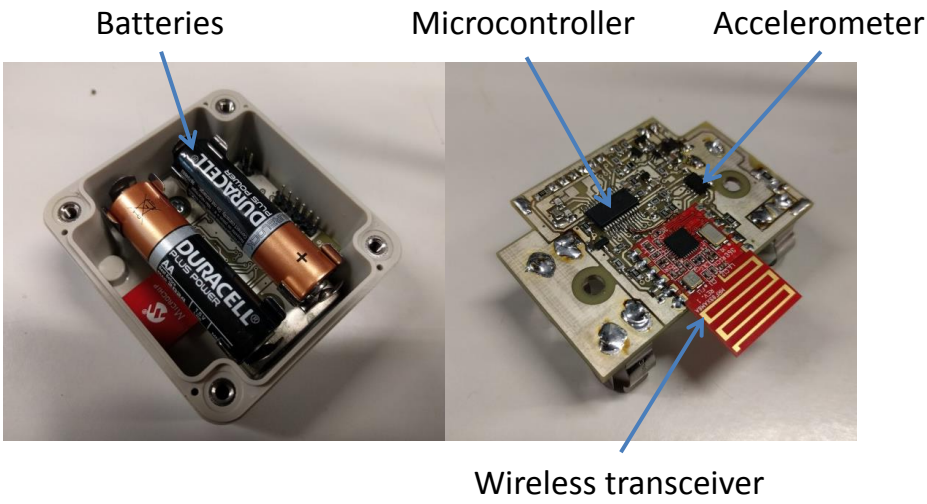

FIGURE 35: INSIDE THE UOB SLEEPER NODE

FIGURE 36: UOB SLEEPER NODE

10.2.3 SYSTEM OUTPUT

The UoB system comprises of four sleeper nodes and one master node. Each sleeper node normally operates in a low power mode, where it briefly measures vertical acceleration every 0.2 s. If the acceleration exceeds a set threshold, the node switches into full measurement mode, where it records the vertical accelerations at 1.6 kSps. This allows accelerations due to a passing train to be recorded. The node will stop recording once the train has passed, or the node's internal memory is full. The node also records its internal temperature and battery voltage whenever a train passes.

Figure 37 shows recorded accelerations from a single train pass, on each of the four UoB nodes. The time axis is measured from the start of each node's recording. It can be seen that each of the nodes start recording at slightly different times. This is due to them triggering at different times.

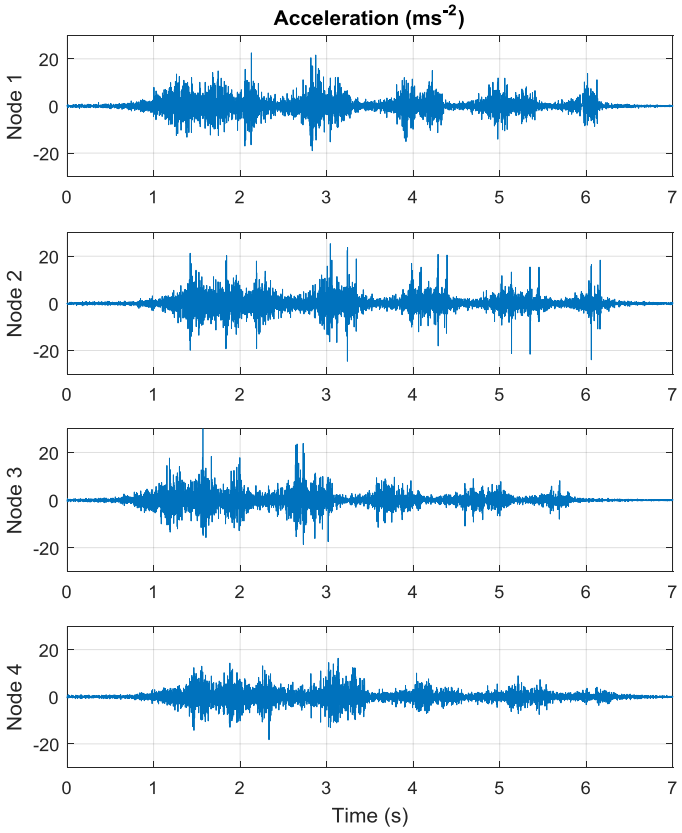

FIGURE 37: ACCELERATIONS MEASURED FROM UOB NODES

Figure 39 shows the calculated displacements from each of the four nodes. Displacements have been calculated by double-integrating the acceleration values, and applying a 2th order high-pass filter with a cut-off frequency of 5 Hz, shown in Figure 38.

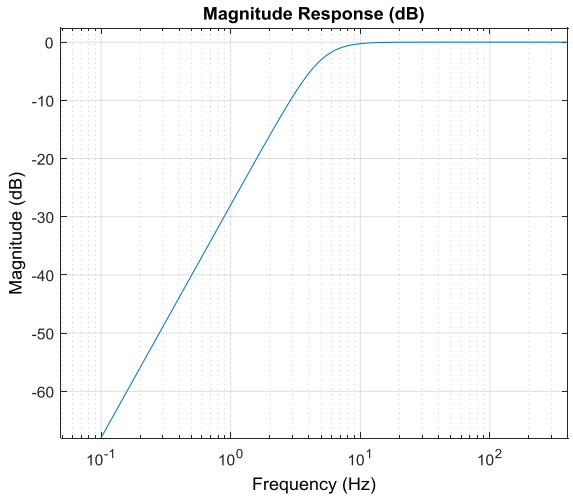

FIGURE 38: 2ND ORDER BUTTERWORTH HIGH-PASS FILTER - FC =5 HZ

In each plot, individual axles of the train are visible, which cause a maximum displacement as they pass over the sleeper. In the plots a positive displacement indicates a downward deflection.

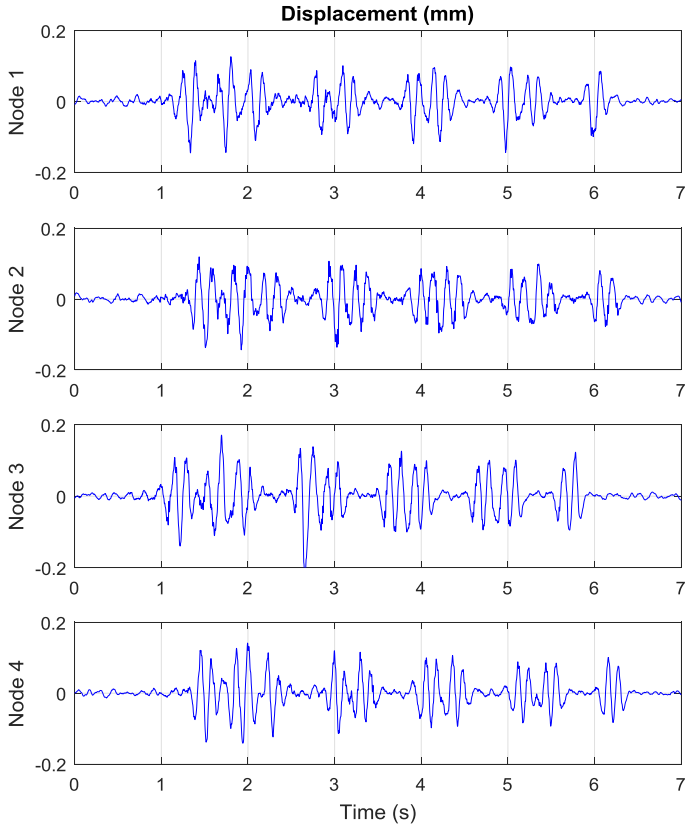

FIGURE 39: DISPLACEMENTS CALCULATED FROM UOB NODE DATA

To monitor the track degradation it is essential that the displacement data are compared with the same train as each train depends on the speed and weight would have a different effect on the displacement of the sleepers. The displacement of the sleepers caused by a passenger train and a freight train are shown Figure 40 and Figure 41 respectively. There is a clear difference in the amplitude of movements. Freight trains typically have highly variable loads on each wheelset whereas a passenger train is much more uniformly loaded.

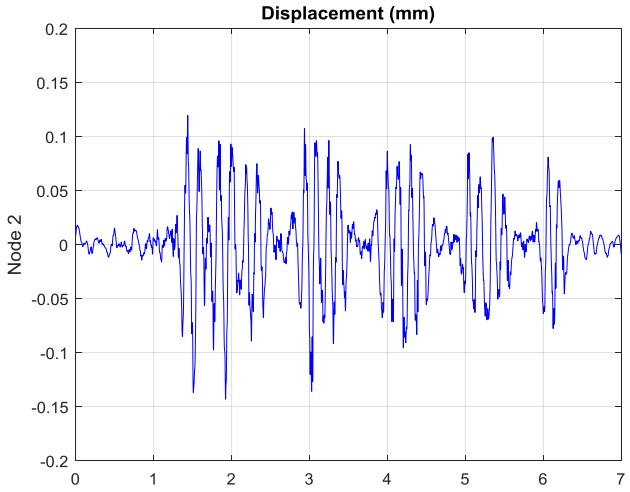

FIGURE 40: DISPLACEMENT CAUSED BY A HIGH-SPEED PASSENGER TRAIN.

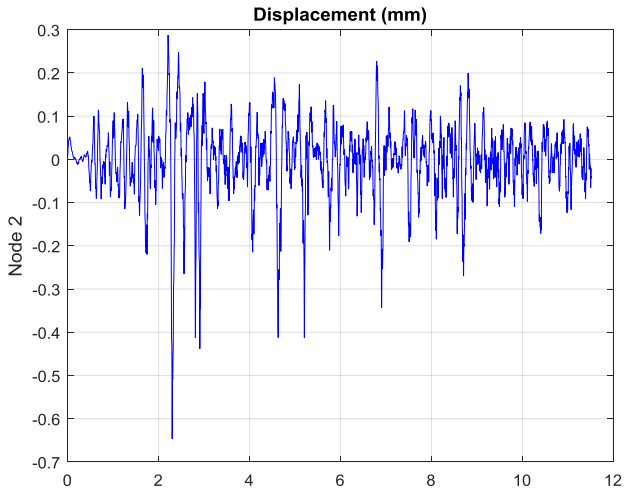

FIGURE 41: DISPLACEMENT CAUSED BY A PART OF A FRIEGHT TRAIN.

10.2.4 CREST FACTOR ANALYSIS

It has been shown that the vibration data can be used to determine the vertical movement of each sleeper. If the sampling rate is chosen correctly, the vibration data can also be used to detect abnormal

behaviour of the rolling stocks such as wheelflats. Wheelflats are usually high impact vibration forces that can appear as a short high amplitude transient the signal. To identify and focus on these impacts a band-pass filter can be applied to the original signal. To determine which frequency band is more efficient to demonstrate these impacts, a crest factor analysis are used in this example.

Crest factor is the ratio of a peak value to the rms value of a signal. For example, the crest factor for a sinusoidal waveform with rms value of one, is 1.414.

A wheelflat impact force creates a relatively high crest factor value. To determine which frequency band contains the most energy of the impact, a spectral analysis of the crest factor is used, shown in Figure 42.

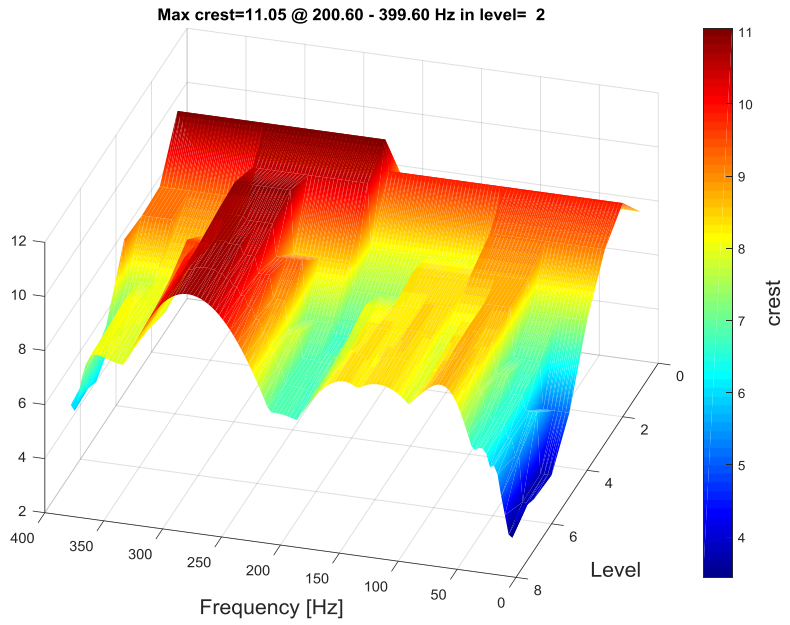

FIGURE 42: CRESTOGRAM OF THE VIBRATION SIGNAL.

This indicates that frequency band around 250-350 Hz contains the highest peaks. After applying this filter to the original signal, the processed signal appears as shown in Figure 43.

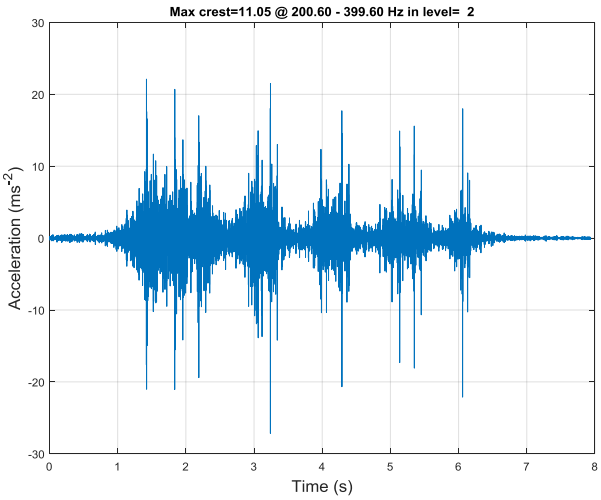

FIGURE 43: VIBRATION SIGNAL AFTER THE BAND-PASS FILTER.

The high peaks in the signal could represent wheelflats. However, this could not be confirmed as this particular line operator currently does not monitor the impact forces.

10.2.5 MONITORING BATTERY VOLTAGE

The UoB accelerometer nodes each report their battery voltage when they record a passing train. Figure 44 shows the battery voltage of a single node over a period of approximately 5 weeks. A repeating cycle is visible within the battery voltage, which coincides with day and night cycles. Figure 45 shows the node temperature recorded with each train pass over the same time period. It can be seen that the temperature inside the node is at its lowest during the night (typically around 10 °C), and rises to a peak during the daytime (typically 30-50 °C). The temperature measured within the node can be higher than the outside air temperature because the node is sealed and continuously exposed to direct sunlight.

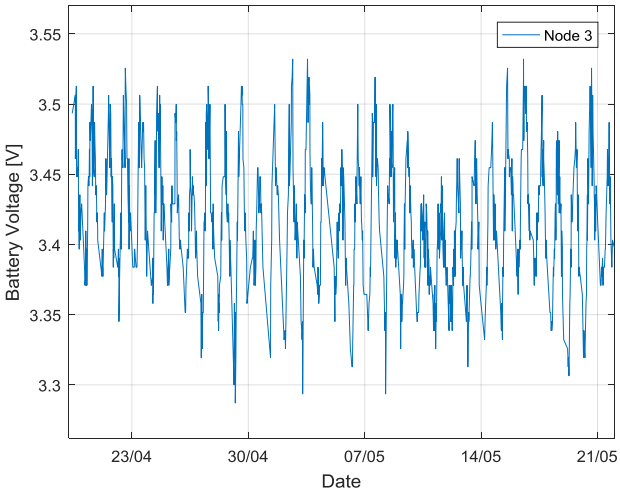

FIGURE 44: NODE BATTERY VOLTAGE FOR EACH TRAIN PASS FOR ~5 WEEKS

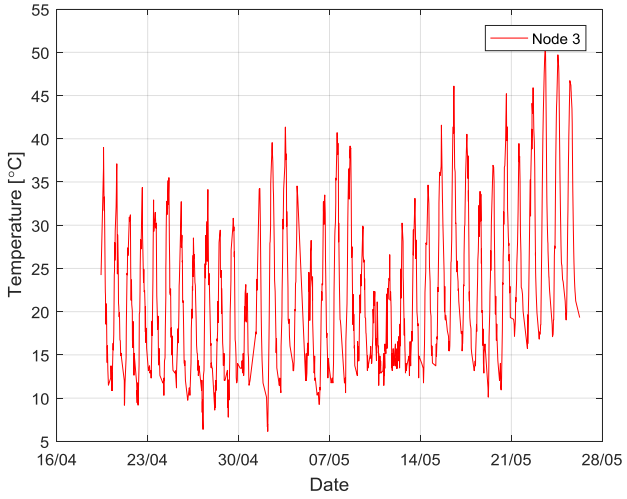

FIGURE 45: NODE TEMPERATURE FOR EACH TRAIN PASS FOR ~5 WEEKS

It was found that the node temperature has an impact on the battery voltage. In Figure 46, battery voltage is plotted against temperature, showing a reasonable correlation between the two.

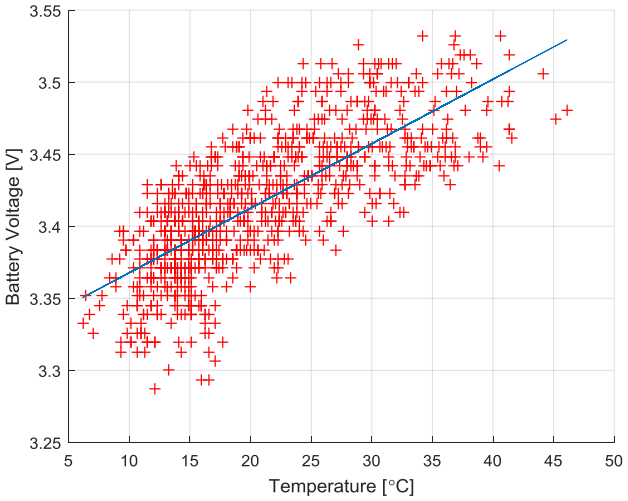

FIGURE 46: NODE BATTERY VOLTAGE VS TEMPERATURE

10.2.6 NODE PROBLEMS

It was found with some of the nodes, that sometimes the battery voltage would drop sharply. Figure 47 shows the battery voltage of one node, showing two sharp drops in voltage between readings.

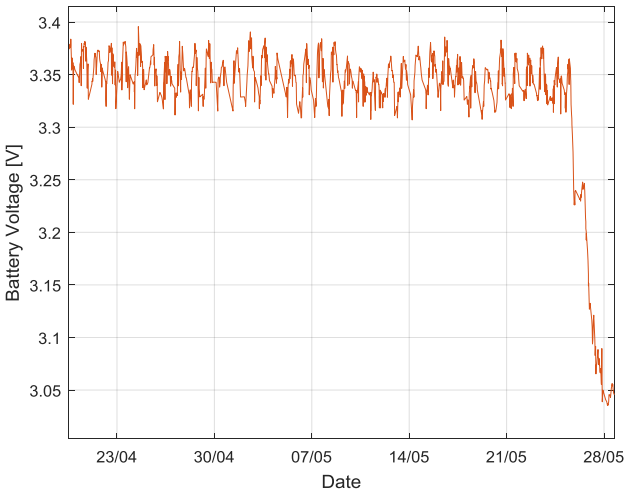

FIGURE 47: NODE BATTERY VOLTAGE SHOWING SHARP DROP

It is speculated that this is due to loss of time synchronisation of the sleeper node. Every hour the sleeper node must synchronise its internal clock with the master node, to allow synchronisation of transmissions and receptions of the short range wireless communications. If the clock synchronisation

fails 6 times in a row (i.e. it has not happened for 6 hours) the sleeper node presumes it must be too far out of sync with the master node. It will then reset itself, and wait indefinitely for a synchronisation signal. This means that the node is continuously using a relatively high amount of power until it receives a valid synchronisation signal. In normal operation, this should occur within one minute, but if a loss of power occurred within the master node, the slave will fail to synchronise until the master is powered up again.

This issue can be corrected with better control communications between the sleeper nodes and the master. The simple synchronisation method used was chosen to keep battery usage to a minimum during normal (problem free) operation.

Another explanation could be that the sleeper node's trigger threshold is set too low so it constantly wakes up to take acceleration measurements, requiring a relatively high power to be consumed for a long time period.

This problem can be corrected by raising the acceleration trigger threshold. Potentially an automatic threshold setting algorithm could be implemented to account for small changes in the accelerometer calibration.

11 Conclusions

This work was carried out to demonstrate how the integration of different technologies can achieve an innovative condition monitoring system for railway application.

A technology marketplace chart, introduced in D4.2.2, was used to identify drivers to design new systems. This document has demonstrated how the integration of diverse technologies can be used to monitor rail movements.

The key points for the design of this system were: low power, energy harvesting, low cost, wireless and easy to install.

The sensing technologies for vibration monitoring were explained and a number of sensors were selected. The selected sensors were assessed through laboratory and field tests.

A low power microcontroller unit was used collect the acceleration data from the vibration sensor. The system also required a method to wirelessly transmit the data. An ISM band low-power wireless module was chosen to locally transmit the data to a central unit at the trackside. Due to the low power consumption, AA-size batteries were used to power each sensing node. Depending on the triggering configuration for each node, the battery life can vary from 1 month to 24 months.

A Raspberry Pi, used within the central unit, was selected as an inexpensive low-power computing system which has a suitable processing power and data storage capacity to process and record measurement data from the sensing nodes. The central unit communicates with the sensing nodes wirelessly using the ISM 900 MHz band. A 3G/4G cellular communication system was also employed to transfer the data and report the results to remote PCs in Porto and Birmingham. To avoid installing additional lineside power infrastructure in order to power the central unit, a use of solar panels was demonstrated. It was identified that the location is suitable for solar energy harvesting and a solar panel with gel batteries were selected to power the computing and communication hardware within the central unit.

A number of wireless and wired standards and technologies have been deployed. Wired standards were used for internal electronic systems and short distance (under 0.5 metre) communications, and short and long range wireless systems were successfully implemented.

In summary, a use of a vibration sensing technology and low power computing systems was shown to have an appropriate applicability to the railway, especially in monitoring of the track.

12 References

[1] Sencieve Ltd, “Wireless Sensor System,” Sencieve, 2016. [Online]. Available: http://www.senceive.com/products/wireless-sensor-system/.

[2] G. J. Yeo, *Monitoring Railway Track Condition Using Inertial Sensors On An In-Service Vehicle,* Birmingham: The University of Birmingham, 2017.

[3] A. L. Robert Neal Dean Jr., “Applications of Microelectromechanical Systems in Industrial Processes and Services,” *IEEE Transactions on Industrial Electronics,* vol. 56, no. 4, pp. 913 - 925, 2009.

[4] “Guite to Accelerometers,” 2016. [Online]. Available: http://www.dimensionengineering.com/info/accelerometers. [Accessed 29 April 2016].

[5] M. Serridge and T. R. Licht, “Piezoelectric accelerometer and vibration amplifierhandbook,” Bruel & Kjaer, Denmark, 1987.

[6] M. Andrejašicˇ, “MEMS Accelerometer,” University of Ljubljana, Slovenia, 2008.

[7] M. Weber, “Vibration Calibrators VC20,” 22 April 2016. [Online]. Available: http://www.mmf.de/manual/vc20mane.pdf.

[8] A. Dewan, S. U. Ay, M. N. Karim and H. Beyenal, “Alternative power sources for remote sensors: A review,” *Journal of Power Sources,* vol. 245, no. 0, pp. 129-143, 2014.

[9] P. Nintanavongsa, “A Survey on RF Energy Harvesting: Circuits and Protocols,” *Energy Procedia,* vol. 56, pp. 414-422, 2014.

[10] S. Bandyopadhyay and A. P. Chandrakasan, “Platform Architecture for Solar, Thermal, and Vibration Energy Combining With MPPT and Single Inductor,” *IEEE Journal of Solid-State Circuits,* vol. 47, no. 9, pp. 2199-2215, 2012.

[11] BP Solar, *Low Energy Remote Power Solutions…,* Marlec Renewable Power, 2006.

[12] “Steca Solsum,” Steca Elektronik GmbH, [Online]. Available: http://www.steca.com/index.php?Steca-Solsum-F-en. [Accessed August 2016].

[13] Victron Energy B.V. , “Gel and AGM Batteries,” [Online]. Available: https://www.victronenergy.com/upload/documents/Datasheet-GEL-and-AGM-Batteries-EN.pdf.

[14] Camdenboss Ltd., "Solar Batteries," [Online]. Available: http://camdenboss.com/batteries/valve-regulated-lead-acid/solar-batteries. [Accessed May 2016].

[15] J. Chou, D. Petrovic and K. Ramachandran, "A distributed and adaptive signal processing approach to reducing energy consumption in sensor networks," *IEEE INFOCOM 2003. Twenty-second Annual Joint Conference of the IEEE Computer and Communications Societies (IEEE Cat. No.03CH37428),* vol. 2, pp. 1054-1062, 2003.

[16] "MRF89XA - Wireless module," Micochip Technology Inc., 2016. [Online]. Available: http://www.microchip.com/wwwproducts/en/MRF89XA.

[17] "AC750 Wireless Dual Band 4G LTE Router," TP-Link, [Online]. Available: http://uk.tp-link.com/products/details/cat-4691_Archer-MR200.html. [Accessed May 2017].

[18] "Cable Lengths and Transmission Speeds," National Instrument, 10 January 2012. [Online]. Available: http://www.ni.com/product-documentation/13724/en/. [Accessed August 2016].